

COST-EFFECTIVE DEFORMATION MONITORING OVER ULTRAWIDE SWATHS USING AMBIGUOUS STAGGERED SAR

Michelangelo Villano¹, Nertjana Ustalli¹, Vinicius Freitas de Almeida², Pau Prats-Iraola¹

¹German Aerospace Center (DLR), Microwaves and Radar Institute, Germany

²Aeronautics Institute of Technology (ITA), Brazil

ABSTRACT

Permanent scatterers interferometry (PSI) is an established technique that enables retrieval of deformations with meter spatial resolution and sub-centimeter accuracy from stacks of synthetic aperture radar (SAR) images. However, the exploitation of this technique for global monitoring places very high demands on the mapping capability of the SAR instrument and mission. Based on the observation that deformation can still be retrieved with similar accuracy even if the SAR images of the stacks are corrupted by significant disturbance, we propose a dedicated ambiguous staggered SAR mode that combines beam shaping in elevation, alternation of orthogonal waveforms, and continuous variation of the pulse repetition interval, and achieves meter resolution over ultrawide ground swaths of over 600 km at a total disturbance level of less than 10 dB. As a result, the mapping capability for deformation monitoring of a satellite like TerraSAR-X can be increased by a factor of up to 20 without any noticeable degradation in performance. The theoretical arguments are supported by analyses of stacks of TerraSAR-X images acquired over Mexico City.

Index Terms—Permanent scatterers interferometry (PSI), ambiguous staggered synthetic aperture radar (SAR), phase-only beam spoiling, orthogonal waveforms, TerraSAR-X.

1. INTRODUCTION

The retrieval of displacements using permanent scatterers interferometry (PSI) is a major application of synthetic aperture radar (SAR). It consists of acquiring a time series of SAR images of a given area, ideally from the same position, detecting temporally stable scatterers, referred to as permanent scatterers (PSs), and exploiting them to estimate local displacements in the line of sight direction with an accuracy in the order of cm or even mm [1]. In contrast to networks of dedicated (satellite-based) navigation ground receivers, it enables the estimation of displacements over large areas, i.e., the area spanned by the SAR images, at spatial resolutions of few meters, namely the resolution of the

SAR images, and thus the detection of possible local anomalies, e.g., a displacement relative to a part of a building.

A mission designed to serve this application on a global scale would require an enormous mapping capability (to cover large areas frequently) together with a very high spatial resolution (to capture local anomalies). Due to the inherent limitation that mutually constrains the swath width and the azimuth resolution in conventional SAR, possible options could be a) resorting to high-resolution wide-swath SAR systems based on digital beamforming (such as ROSE-L, ALOS-4 or NISAR), which are effective but complex and expensive, or b) deploying constellations of low-cost NewSpace SAR systems, which are, however, so far limited in terms of orbit duty cycle, swath width and orbit control accuracy.

In recent years, novel ambiguous SAR modes have been devised that overcome the aforementioned inherent limitation and enable high-resolution SAR imaging of wide swaths – without the need for digital beamforming – at the cost of increased disturbance from thermal noise and ambiguities [2]. In particular, the ambiguous staggered SAR mode consists of transmitting pulses with variable pulse repetition interval (PRI) over a wide swath with a mean PRI much shorter than that required in stripmap, and collect all echoes with a wide receiving beam. This mode is attractive due its negligible azimuth ambiguities and blurred (range) ambiguities, which make it ideal for detecting strong targets, such as ships, and has indeed been proven effective for maritime surveillance through experimental TerraSAR-X demonstrations, where ground swaths of up to 160 km have been mapped with an azimuth resolution of about 2 m [3], [4].

In this work, we discuss the adaptation of the ambiguous staggered SAR mode to deformation monitoring and evaluate the maximum swath that can be attained with negligible performance degradation. TerraSAR-X is used as a case study, but the discussion is general and applicable to any conventional phased-array SAR system.

2. AMBIGUOUS STAGGERED SAR FOR DEFORMATION MONITORING

The ambiguous staggered SAR mode for deformation monitoring should be characterized by the following features:

- *Ultrawide elevation beam on transmit and receive with increasing gain from near to far range.* The beam shall cover the full swath to be imaged and the gain trend should guarantee an approximately constant noise-equivalent sigma zero (NESZ) across the swath. In phased-array SAR systems, such a beam can be obtained – without compromising transmitted power – through phase-only beam spoiling, as proposed in [5]. Fig. 1 shows two examples of normalized one-way elevation pattern achievable for TerraSAR-X, which would allow mapping ultrawide swaths of 300 km (left) and 600 km (right) with approximately constant NESZ. The resulting ripple will be accounted for in the analysis;
- *Continuous PRI variation.* This is required to avoid blind ranges. The sequence can be designed according to the criteria defined for staggered SAR (see [6]), whereby missing consecutive samples in azimuth should be avoided, but is not critical. The mean PRI of the system should be in the order of or slightly smaller than that required by the antenna length. A desired side effect of the PRI variation is the blurring of range ambiguities and nadir echoes;
- *Alternation of orthogonal waveforms.* It is advised to employ a set of orthogonal waveforms, e.g., defined as in [7], to further blur range ambiguities and nadir echoes. The number of orthogonal waveforms of the set should be equal or higher than the number of range ambiguities within the swath. The orthogonality is here assumed for point targets.

3. ACHIEVABLE SWATH WIDTH AND EXPECTED PERFORMANCE

The maximum achievable swath width and the expected performance are assessed under the assumption that the total disturbance resulting from thermal noise, clutter, and ambiguities has additive white Gaussian noise (AWGN) characteristics. This assumption can be justified considering that the unambiguous clutter becomes negligible as the swath increases and the ambiguous clutter, resulting from range ambiguities, has AWGN characteristics due to the use of PRI variation and orthogonal waveforms [6], [7].

The total disturbance level of an image acquired in ambiguous staggered SAR mode therefore results from thermal noise and ambiguities. Let us define as $NESZ^*$ and W_g^* the nominal NESZ and swath width of the system in stripmap mode ($NESZ^* = -22$ dB, $W_g^* = 30$ km for TerraSAR-X). Under the assumption that the elevation pattern guarantees an approximately constant NESZ across the swath, it can be shown that the NESZ obtained for a swath $W_g \gg W_g^*$ can be approximated as [8]

$$NESZ \cong 4 NESZ^* \left(\frac{W_g}{W_g^*} \right)^2 \quad (1)$$

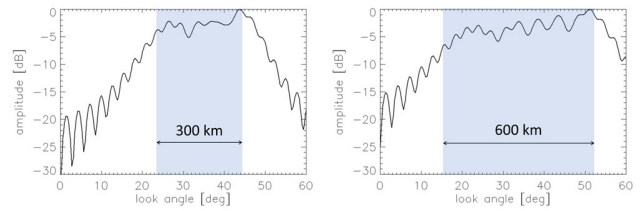


Fig. 1. Examples of normalized one-way elevation patterns obtained using phase-only beam spoiling to map an ultrawide swath of 300 km (left) and 600 km (right) with approximately constant NESZ.

where the conservative factor 4 accounts for possible losses due to the presence of ripple in the elevation pattern.

As for the ambiguous clutter, we introduce the ambiguity-equivalent sigma zero (AESZ), which can be approximated – always under the assumption that the elevation pattern guarantees an approximately constant NESZ across the swath – as the product of the number of range ambiguities N_{amb} and the mean backscatter of the imaged area σ_{mean} [8]:

$$AESZ \cong N_{amb} \sigma_{mean} \quad (2)$$

As the returns from the region between the nadir and the near range might not be attenuated enough (see patterns in Fig. 1), we conservatively include in N_{amb} all range ambiguities coming from nadir till far range (it is in any case fundamental to avoid that nadir echoes determine receiver saturation):

$$N_{amb} = \left\lfloor \frac{R_F - h}{c_0} PRF_{mean} \right\rfloor \quad (3)$$

where R_F is far range, h is the range to nadir, c_0 is the speed of light and PRF_{mean} is the reciprocal of the mean PRI.

Fig. 2 shows the disturbance level of ambiguous staggered SAR as a function of the swath width for TerraSAR-X, assuming $PRF_{mean} = 3525$ Hz and $\sigma_{mean} = -8$ dB (please note that this is a very conservative assumption for the mean backscatter of an area of several hundreds of km^2) [9]. An antenna tilt of 33.8° is assumed and the maximum displayed swath (635 km) corresponds to a minimum incidence angle of 15° . The total disturbance is about 5 dB for a 300-km swath and less than 10 dB for a 600-km swath. The noise and ambiguity components are highlighted in red and blue, respectively. In this example, thermal noise dominates over ambiguities for swaths larger than 130 km.

The outcome of this analysis allows deriving the PSs detection performance under the assumption that PSs are modeled as Swerling 0 targets (constant amplitude) occupying a single resolution cell and that the disturbance has AWGN characteristics. Defining the dispersion index as the ratio of the standard deviation and the mean of the amplitude across the time series, Fig. 3 shows the false alarm rate (i.e., the probability of identifying disturbance as a PS) as a function of the dispersion index threshold (a PSs is detected,

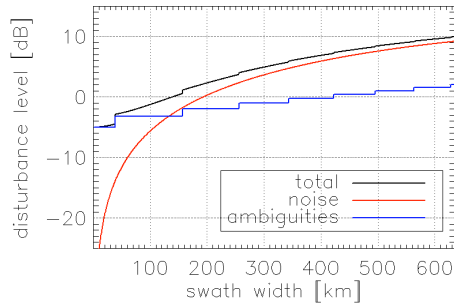


Fig. 2. Disturbance level of ambiguous staggered SAR as a function of the swath width for TerraSAR-X. The noise and ambiguity components are highlighted in red and blue, respectively.

if the dispersion index is below the threshold) for different number of images of the stack N . Ensuring a false alarm rate of, e.g., 10^{-7} , which corresponds to 1 false alarm every 100 km² for 10 m² spatial resolution, requires a dispersion index threshold of 0.3 and 0.25 for a stack of 60 and 45 images, respectively.

Fig. 4 shows the detection probability of PSs with signal-to-disturbance ratio of 8 dB. It can be noticed that for a dispersion index threshold of 0.3 (which was required to ensure the desired false alarm rate for $N = 60$), a detection probability of over 0.9 is achieved for $N = 60$. The detection probability for the same signal-to-disturbance ratio and false alarm rate becomes lower for smaller values of N , e.g., 0.3 for $N = 45$ (dispersion index threshold of 0.25). Depending on the amplitude distribution of the PSs present in the specific scene, a larger number of false alarms could be accepted (by adopting a higher threshold) to detect more PSs.

4. RESULTS FROM PROCESSING STACKS OF TERRASAR-X IMAGES OVER MEXICO CITY

In order to demonstrate the potentialities of the ambiguous staggered SAR mode a stack of 45 TerraSAR-X images (with ~ 3 m spatial resolution) acquired over Mexico City, Mexico, in the time span May 2011 – February 2015 have been analyzed. This area is known to be characterized by notable deformation rates in the order of few cm/month.

As a first step, we have performed PSs detection over the original stack with a dispersion index threshold of 0.2 using the processing tool TAXI [10]. 460346 PSs have been detected over an area of approximately 210 km². Fig. 5 shows a histogram of the mean amplitude of the PSs in dB, which spans an interval of almost 40 dB. The signal-to-disturbance ratio (in dB) used for the detection performance in Section 3 is obtained by subtracting the mean amplitude (in dB) and the total disturbance (in dB) derived in Section 2.

We have artificially deteriorated the quality of all images by adding noise with AWGN characteristics, corresponding to total disturbance levels of 5 dB and 10 dB, respectively,

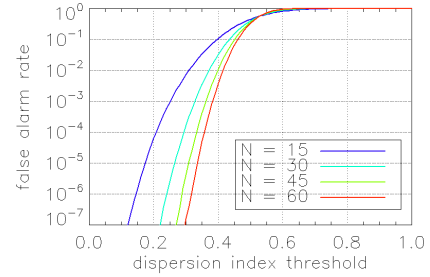


Fig. 3. False alarm rate as a function of the dispersion index threshold for different number of images of the stack N .

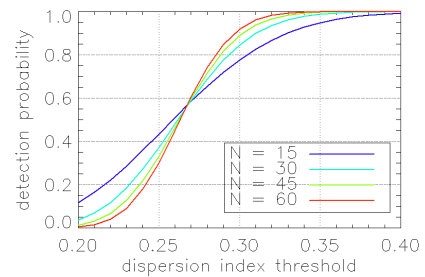


Fig. 4. Detection probability of PSs with signal-to-disturbance ratio of 8 dB as a function of the dispersion index threshold for different number of images of the stack N .

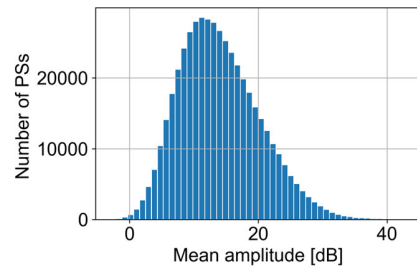


Fig. 5. Histogram of the mean amplitude (1-dB step) of PSs detected in a stack of 45 TerraSAR-X images acquired over Mexico City, Mexico.

and reprocessed the data. It is important to point out that the noise has been added to the images before coregistration. Some analyses of PSI using deteriorated images have been recently reported in [11].

In the top panels of Fig. 6 the multi-temporal SAR images are shown with disturbance levels of -22 dB (no deterioration), 5 dB, and 10 dB, respectively, while in the bottom panels the resulting deformation rate obtained for the three aforementioned disturbance levels are displayed, where dispersion index thresholds of 0.2, 0.3 and 0.4 have been used, respectively. It can be noticed that the mean deformation velocity is almost fully captured, even for stacks of very noisy images, which would be acquired in ambiguous staggered SAR mode for swath width of over 600 km.

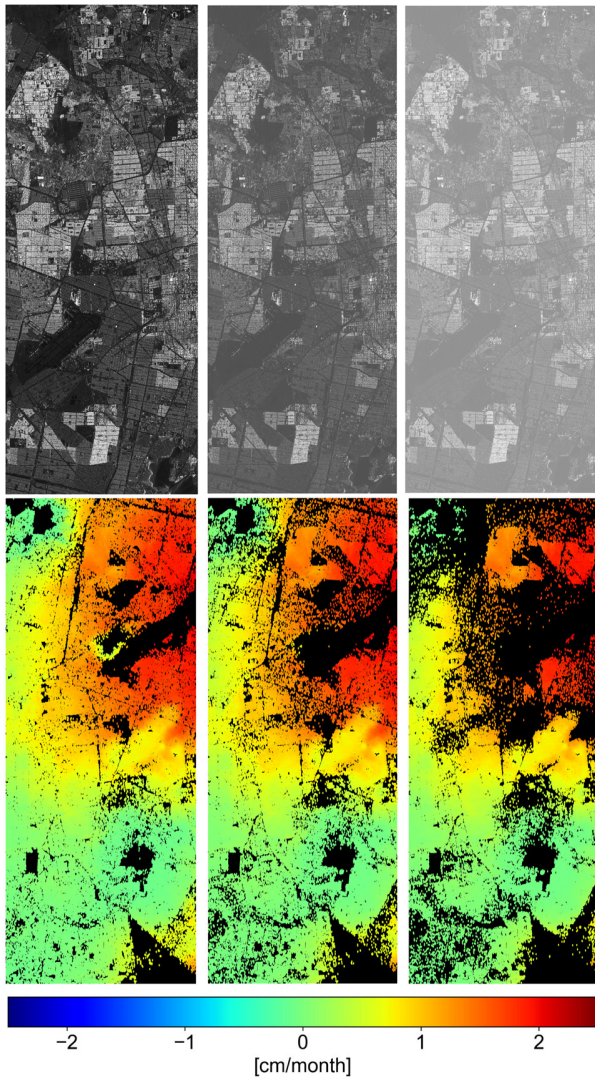


Fig. 6. Multi-temporal SAR images (top) and resulting mean deformation velocity (bottom) for disturbance levels of -22 dB (no deterioration, left), 5 dB (center) and 10 dB (right).

5. CONCLUSIONS

This work promotes the ambiguous staggered SAR mode as an effective solution to monitor deformation at global scale. The analyses, based on several conservative assumptions and results from the processing of a stack of TerraSAR-X images, show that the mapping capability of a system like TerraSAR-X could be extended by a factor of up to 20, while still ensuring the desired performance for deformation monitoring. Further performance improvement can be obtained by partially removing the ambiguous clutter through multi-focus postprocessing [12]. Demonstration of the mode, e.g., using TerraSAR-X, although requiring significant time and resources, would pave the way to a new strategy for cost-effective monitoring of our dynamic Earth, based on frequent, low-quality SAR observations.

ACKNOWLEDGEMENTS

This work was partially funded by the European Union (ERC, DRITUCS, 101076275). Views and opinions expressed are however those of the authors only and do not necessarily reflect those of the European Union or the European Research Council Executive Agency. Neither the European Union nor the granting authority can be held responsible for them.

REFERENCES

- [1] A. Ferretti, C. Prati and F. Rocca, "Permanent scatterers in SAR interferometry," *IEEE Trans. Geosci. Rem. Sens.*, vol. 39, no. 1, pp. 8-20, Jan. 2001.
- [2] N. Ustalli and M. Villano, "High-resolution wide-swath ambiguous synthetic aperture radar modes for ship monitoring," *Remote Sens.*, vol. 14, no. 13, p. 3102, Jun. 2022.
- [3] N. Ustalli, M. N. Peixoto, T. Kraus, U. Steinbrecher, G. Krieger and M. Villano, "Experimental Demonstration of Staggered Ambiguous SAR Mode for Ship Monitoring with TerraSAR-X," *IEEE Trans. Geosci. Remote Sens.*, vol. 61, pp. 1-16, 2023.
- [4] N. Ustalli, M. Nogueira Peixoto, T. Kraus, U. Steinbrecher, G. Krieger and M. Villano, "Experimental Demonstration of Ambiguous Staggered SAR with Waveform Alternation for Coastal Surveillance," *IEEE Geosci. Rem. Sens. Lett.*, vol. 21, pp. 1-5, 2024.
- [5] M. Villano, G. Krieger and A. Moreira, "Advanced spaceborne SAR systems with planar antenna," *Proc. 2017 IEEE Radar Conference*, Seattle, WA, USA, 2017, pp. 0152-0156.
- [6] M. Villano, "Staggered synthetic aperture radar," Ph.D. dissertation, Karlsruhe Inst. Technol., Weßling, Germany, 2016.
- [7] W.-Q. Wang, "Mitigating Range Ambiguities in High-PRF SAR With OFDM Waveform Diversity," *IEEE Geosci. Rem. Sens. Lett.*, vol. 10, no. 1, pp. 101-105, Jan. 2013.
- [8] M. Villano, N. Ustalli, V. Freitas de Almeida and P. Prats, "Cost-Effective Global Deformation Monitoring Using Ambiguous Staggered SAR and Permanent Scatterer Interferometry," *IEEE Geosci. Rem. Sens. Lett.*, vol. 22, pp. 1-5, 2025.
- [9] P. Rizzoli, "Radar Backscatter Modeling Based on Global TanDEM-X Mission Data," Ph.D. dissertation, Karlsruhe Inst. Technol., Weßling, Germany, 2018.
- [10] P. Prats et al., "Taxi: A versatile processing chain for experimental TanDEM-X product evaluation," *2010 IEEE IGARSS*, Honolulu, HI, USA, 2010, pp. 4059-4062.
- [11] J. Krecke et al., "Performance Simulation of SmallSat SAR Persistent Scatterer Interferometry With Deteriorated Images," *IEEE Geosci. Rem. Sens. Lett.*, vol. 22, pp. 1-5, 2025.
- [12] M. Villano, G. Krieger and A. Moreira, "Waveform-Encoded SAR: A Novel Concept for Nadir Echo and Range Ambiguity Suppression," *EUSAR 2018; 12th European Conference on Synthetic Aperture Radar*, Aachen, Germany, 2018, pp. 1-6.